

# One-Step Electrospinning of Cross-Linked Chitosan Fibers

Jessica D. Schiffman and Caroline L. Schauer\*

Department of Materials Science and Engineering, Drexel University, Philadelphia, Pennsylvania 19104

Received June 22, 2007; Revised Manuscript Received July 24, 2007

Chitin is a nitrogen-rich polysaccharide that is abundant in crustaceans, mollusks, insects, and fungi and is the second most abundant organic material found in nature next to cellulose. Chitosan, the *N*-deacetylated derivative of chitin, is environmentally friendly, nontoxic, biodegradable, and antibacterial. Fibrous mats are typically used in industries for filter media, catalysis, and sensors. Decreasing fiber diameters within these mats causes many beneficial effects such as increased specific surface area to volume ratios. When the intrinsically beneficial effects of chitosan are combined with the enhanced properties of nanofibrous mats, applications arise in a wide range of fields, including medical, packaging, agricultural, and automotive. This is particularly important as innovative technologies that focus around bio-based materials are currently of high urgency, as they can decrease dependencies on fossil fuels. We have demonstrated that Schiff base cross-linked chitosan fibrous mats can be produced utilizing a one-step electrospinning process that is 25 times faster and, therefore, more economical than a previously reported two-step vapor-cross-linking method. These fibrous mats are insoluble in acidic, basic, and aqueous solutions for 72 h. Additionally, this improved production method results in a decreased average fiber diameter, which measures  $128 \pm 40$  nm. Chemical and structural analyses were conducted utilizing Fourier transform infrared spectroscopy, solubility studies, and scanning electron microscopy.

Innovative technologies focused around bio-based materials are currently of high urgency as they can decrease dependencies on fossil fuel.<sup>1</sup> Chitin is the second most abundant organic material found in nature, from which the *N*-deacetylated derivative chitosan can easily be obtained. Current harvesting primarily utilizes crab and shrimp shells discarded by the canning industries; however, there exists a sizable economic feasibility of growth potential since chitin is also found in fungi, insects, and yeast.<sup>2</sup>

The intrinsically enticing properties of chitosan such as antibacterial activity, biodegradability, and biocompatibility<sup>3</sup> paired with the fact that it is a readily available renewable resource<sup>4</sup> make chitosan the ideal candidate for uses in a wide range of industries, including ophthalmology, medicine, agriculture, textiles, paper coatings, and automotive.<sup>2,5–9</sup>

Electrospinning is an inexpensive, effective, and simple method of producing non-woven nanofibrous mats, which intrinsically have  $10^3$  times larger specific surface to volume ratios, increased flexibility in surface functionalities, improved mechanical performances, and smaller pores than fibers produced using traditional methods.<sup>10–12</sup> The necessary components of an electrospinning apparatus include a high power voltage supply, a capillary tube with a needle or pipet, and a collector that is usually composed of a conducting material.<sup>10</sup> The collector is held at a relatively short distance from the capillary tube, which contains a polymeric solution connected to the high power supply. Pendant droplets of polymer solution are initially held in place in the capillary tube due to surface tension. However, at a critical voltage, a conical protrusion, commonly referred to as a Taylor Cone,<sup>13</sup> is formed.<sup>14</sup> From this, a nearly straight jet emerges and travels for a few centimeters. At the end of this segment, the jet takes on a diaphanous and conical shape, within which exists the complicated path taken by the jet.<sup>15</sup> While the jet is moving conically, it experiences bending instabilities and its field is directed toward the collector, which

is oppositely charged. By the time the jet reaches the collector, the solvent evaporates, thus dry polymer fibers are deposited on the collector.<sup>5</sup> All currently observed polymer jets have been theoretically and experimentally observed to be continuous; therefore, electrospinning creates seemingly endless ultrafine fibers that collect in a random pattern.<sup>15,16</sup> Fibrous mats are utilized in the aforementioned fields that chitosan could be used in. Additionally, electrospinning researchers envision the mats in other areas such as filter media, catalysis, protective clothing, cosmetics, sensors, nanocomposites, and tissue engineering.<sup>2,10</sup> More specifically, because of the biofunctionality and biocompatibility of the biopolymer, electrospun chitosan could be used to improve tissue engineering scaffolds by increasing their cytocompatibility while also mimicking the native extracellular matrix.<sup>17</sup>

Glutaraldehyde (GA) has been demonstrated to cross-link chitosan through two main mechanisms. One method is Schiff base formation, which has cross-linking that results in imine-type functionality.<sup>18,19</sup> The second method is Michael-type adducts with terminal aldehydes that lead to the formation of carbonyl groups.<sup>18,20</sup>

Recently, it has been demonstrated<sup>21</sup> that solutions of low, medium, and high molecular weight, as well as a practical grade of chitosan dissolved in trifluoroacetic acid (TFA), can be electrospun without purification or additional polymers or solvents into randomly oriented, continuous, bead-free fibers. A post-production procedure featuring vapor-phase GA can be taken to effectively cross-link the fiber mats utilizing a Schiff base imine functionality. This method of creating cross-linked chitosan fibers is a two-step method: fiber production followed by fiber exposure to vapor-phase GA for 24 h.

Currently, we are demonstrating that cross-linked chitosan fibers can be produced utilizing a one-step production method instead of the previously reported two-step method. Here, a 50 wt % GA/water solution is added to the chitosan/TFA system just prior to spinning. The cross-linking occurs during the time

\* Corresponding author. E-mail: cschauer@cbis.ece.drexel.edu.

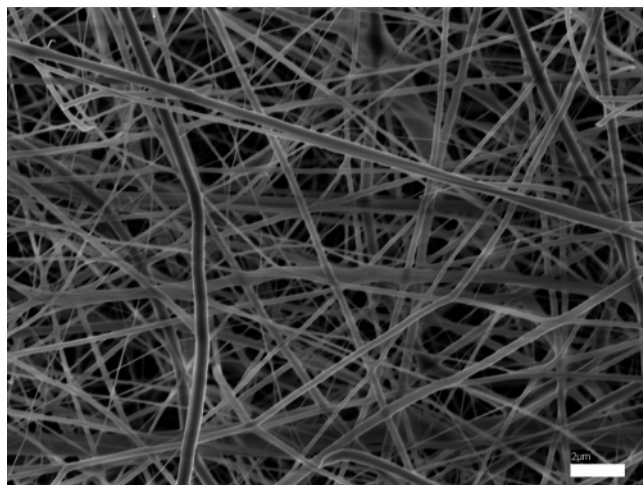


**Figure 1.** SEM image of electrospun one-step cross-linked chitosan fibers. A 2  $\mu\text{m}$  marker is displayed.

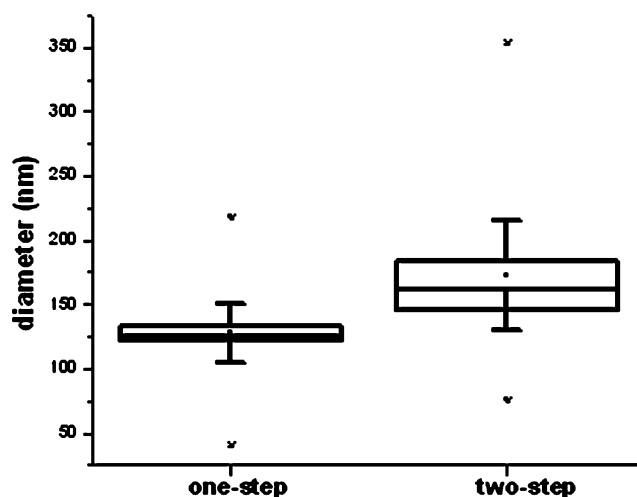


**Figure 2.** Box plots displaying the diameter size distribution of cross-linked electrospun chitosan fibrous mats produced using the one-step cross-linking method (left) and two-step cross-linking method (right). The mean and median fiber diameters observed are represented in the box plots by the square inside the box and the line inside the box, respectively.

it takes to electrospin. The implementation of a one-step as opposed to a two-step production method would lower manufacturing costs and production times for all applications where chitosan fiber mats would be used. Hence, this reactive electrospinning method could bring chitosan nanofibrous mat technology closer to being implemented for large-scale production.

Figure 1 is a scanning electron microscope (SEM) micrograph, which demonstrates that cylindrical, randomly oriented, continuous fibers are created using the one-step fiber production technique. There is a 2  $\mu\text{m}$  marker displayed in the lower right corner of the image.

Average fiber diameter was determined by averaging the diameter of 50 random fibers. Figure 2 displays the average fiber size distributions for the cross-linked chitosan fibers produced by the one-step method (left) and the two-step method (right). The box outline is the standard error. The square inside the box is the mean data point, and the line inside the box is the median data location; this box and line respectively refer to the mean fiber diameter and median fiber diameter observed. The whiskers display the upper inner and lower inner fence values. The upper inner fence whisker extends to the 75th

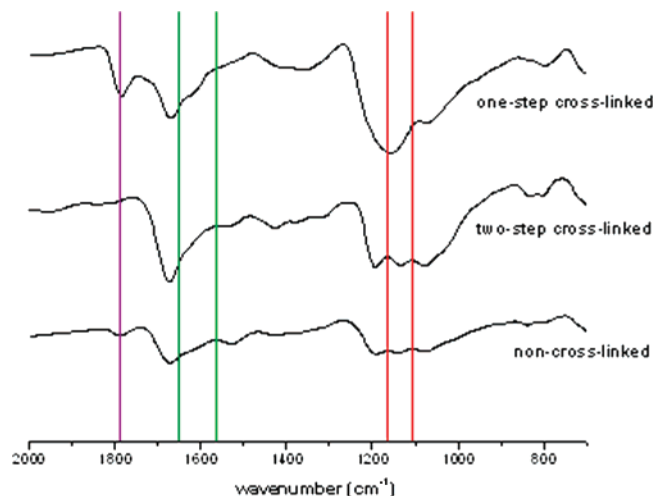


**Figure 3.** FTIR spectra of electrospun non-cross-linked (bottom), two-step cross-linked (middle), and one-step cross-linked chitosan fibers (top). The purple line (1790  $\text{cm}^{-1}$ ) indicates the location of a carboxylic acid. The green lines (dark at 1650  $\text{cm}^{-1}$  and bright at 1560  $\text{cm}^{-1}$ ) exhibit changes due to a Schiff base functionality. The red lines indicate that only the one-step method experiences a shift in the alcohol regions.

percentile plus 1.5 times the interquartile range, while the lower inner fence value extends down to the 25th percentile minus 1.5 times the interquartile range. Above and below the whiskers, a “+” indicates the maximum/minimum data point and “x” indicates the first/99th percentile (these values appear to overlap in the figure). Hence, the largest and smallest fiber diameter observed are also representative of the outer bounds of almost all of the fiber diameters observed. Data points that lie outside the fence values are considered outliers. Outliers and individual data points were not plotted on the provided box plots.

The average diameter for one-step cross-linked chitosan fibers was found to be  $128 \pm 40$  nm. To illustrate the range, the smallest and largest fiber diameters measured were 40 and 218 nm, respectively. Previously reported<sup>21</sup> average fiber diameters for non-cross-linked and two-step cross-linked chitosan fibers were found to be  $77 \pm 29$  nm and  $172 \pm 75$  nm respectively. It is of interest to note that the average one-step cross-linked fiber diameters are larger than non-cross-linked fibers, but smaller than two-step cross-linked fibers. Therefore, the one-step cross-linking method produces faster cross-linked chitosan fibers with smaller average fiber diameters relative to those produced when the vapor-GA two-step method was employed.

Figure 3 displays the Fourier transform infrared spectroscopy (FTIR) spectra of non-cross-linked (bottom), two-step cross-linked (middle), and one-step cross-linked (top) chitosan fibers, which were directly evaluated by attenuated reflectance utilizing whole fibers. The non-cross-linked and the one-step cross-linked chitosan fibers distinctly display a peak (Figure 3, purple line) at 1790  $\text{cm}^{-1}$  and 1786  $\text{cm}^{-1}$  respectively, indicating the presence of a carboxylic acid. The origin of this is from the TFA used to electrospin the fibers. In the electrospinning process, there exists a rapid solvent evaporation as well as phase separation as the polymer solution jet is thinned.<sup>5</sup> However, it is possible that, if the solvent utilized is not volatile enough for the chosen process parameters, some solvent will remain in the fibers post-electrospinning. The spectra for the two-step cross-linked fibers fail to exhibit the carboxylic acid as distinctly. It is possible that there exists a solvent exchange between the vapor-GA and the remaining TFA since either the solvent is hydrogen bound to the fibers or the amine on the chitosan is

protonated by TFA. Therefore, the remaining anion of the TFA acetate is associated with the positively charged polymer. Cross-linking during fiber production might lead to enhanced interactions of the TFA and GA since they are effectively acting as a single solvent solution.

The spectral changes previously observed due to two-step cross-linking were again observed when the one-step cross-linking method was utilized. However, significant yet expected additional changes were also observed. As noted earlier, there are two main cross-linking mechanisms. Previously, two-step cross-linking of chitosan nanofibers only experienced the Schiff base mechanism. This method is characterized by a change in the carbonyl-amide region. The split peak at  $1650\text{ cm}^{-1}$  (Figure 3, dark green line) is the location of the new C=N imine that has been noted to occur between  $1620$  and  $1660\text{ cm}^{-1}$ . The peak observed in the non-cross-linked chitosan fibers at  $1560\text{ cm}^{-1}$  (the bright green line in Figure 3) disappear in both cross-linked fiber spectra, thus indicating a Schiff base imine functionality due to a loss of the free amines.<sup>18</sup> One-step cross-linking is consistent with the two-step process because, again, Michael-type cross-linking, which would be identified by carbonyl groups in the  $1720\text{--}1730\text{ cm}^{-1}$  region is not observed.

However, there is a major apparent difference between the one-step cross-linked fibers and the other spectra in the primary and secondary alcohol region (Figure 3, red lines). A possible explanation for this is the increased interactions of the TFA with the GA as a single solution when implemented in the one-step cross-linking process.

After the GA liquid is added to the polymer solution to be electrospun, no agglomeration, gelation, or other issues that might infringe on the electrospinning process were experienced. Typically, 4 mL of polymer solution was loaded and electrospun at a rate of 1.2 mL/h; thus the syringe was emptied in approximately 3.33 h. Within this time frame, again, no agglomeration of the solution was observed. By the completion of an electrospinning session, the deposited fibers changed from white to yellow. Excess solution sitting under the chemical hood also experienced a slight deepening in color from a tan to light yellow. Taul<sup>18</sup> et al. observed the same color change that the fibrous mats experienced during the electrospinning process. They attributed the change to the creation of conjugated double bonds in the structure. Additionally, it was observed that solutions stored in the refrigerator overnight turned brown. No attempts at electrospinning brown solutions were made; however, these solutions did not appear to be completely gelled. In our next set of experiments, we will evaluate the time dependencies that cross-linking with GA liquid has on the polymeric solution, both when used in one-step cross-linking, and when applied as a vapor in two-step cross-linking.

Previous solubility testing of  $2.54\text{ cm} \times 1.27\text{ cm}$  non-cross-linked chitosan fibrous mats demonstrated that, when subjected to acidic acid and ultrapure water solutions, instantly all structural and mechanical properties are lost. Fibrous mats subjected to sodium hydroxide (NaOH) solutions demonstrated shape and color (white) retention for both the 15 min and 72 h tests. In order for electrospun chitosan fiber mats to be implemented in a larger range of applications, the mats must

have an increased structural integrity, hence cross-linking was investigated. It was determined that the solubility of the one-step cross-linked chitosan fiber mats exhibited the same responses when immersed in acetic acid, ultrapure water, and NaOH solutions that the two-step cross-linked chitosan fibers exhibited. The one-step cross-linked fiber mats survived the acetic acid, water, and NaOH solutions for 15 min as well as 72 h. After the fiber mats were removed from the solutions, visual inspection implied that their rigidity and shape were unaltered. Additionally, their yellow color was retained.

In conclusion, in one step, Schiff base cross-linked chitosan fiber mats can be produced quicker and with smaller average diameters than if manufactured using a two-step vapor method.

**Acknowledgment.** This work was funded by NSF IGERT (DGE-0221664) and by Graduate Assistance in Areas of National Need-Drexel Research and Education in Advanced Materials (GAANN-DREAM) (P200A060117), which is funded by the Department of Education's Office of Postsecondary Education.

**Supporting Information Available.** Methods and Materials. This material is available free of charge via the Internet at <http://pubs.acs.org>.

## References and Notes

- (1) Mohanty, A. K.; Misra, M.; Drzal, L. T. *J. Polym. Environ.* **2002**, *10* (1/2), 19–26.
- (2) Kumar, M. N. V. R. *React. Funct. Polym.* **2000**, *46* (1), 1–27.
- (3) Rinaudo, M. *Prog. Polym. Sci.* **2006**, *31* (7), 603–632.
- (4) Kaplan, D. L. *Biopolymers From Renewable Resources*; Springer: New York, 1998; p 417.
- (5) Subbiah, T.; Bhat, G. S.; Tock, R. W.; Parameswaran, S.; Ramkumar, S. S. *J. Appl. Polym. Sci.* **2005**, *96* (2), 557–569.
- (6) Berger, J.; Reist, M.; Mayer, J. M.; Felt, O.; Peppas, N. A.; Gurny, R. *Eur. J. Pharm. Biopharm.* **2004**, *57*, 19–34.
- (7) Chirkov, S. N. *Appl. Biochem. Microbiol.* **2002**, *38* (1), 1–8.
- (8) Dodane, V.; Vilivalam, V. D. *Pharm. Sci. Technol. Today* **1998**, *1* (6), 246–253.
- (9) Vartiainen, J.; Motion, R.; Kulomen, H.; Ratto, M.; Skytta, E.; Ahvenainen, R. *J. Appl. Polym. Sci.* **2004**, *94*, 986–993.
- (10) Huang, Z.-M.; Zhang, Y. Z.; Kotaki, M.; Ramakrishna, S. *Compos. Sci. Technol.* **2003**, *63* (15), 2223–2253.
- (11) Formhals, A. Process and apparatus for preparing artificial threads. U.S. Patent 1,975,504, 1934.
- (12) Reneker, D. H.; Chun, I. *Nanotechnology* **1996**, *7*, 216–223.
- (13) Taylor, G. *Proc. R. Soc. London, Ser. A* **1964**, *280* (1382), 383–397.
- (14) Shin, Y. M.; Hohman, M. M.; Brenner, M. P.; Rutledge, G. C. *Polymer* **2001**, *42* (25), 09955–09967.
- (15) Reneker, D. H.; Yarin, A. L.; Fong, H.; Koombhongse, S. *J. Appl. Polym. Sci.* **2000**, *87* (9), 4531–4547.
- (16) Baumgarten, P. K. *J. Colloid Interface Sci.* **1971**, *36* (1), 71–79.
- (17) Pham, Q. P.; Sharma, U.; Mikos, A. G. *Tissue Eng.* **2006**, *12* (5), 1197–1211.
- (18) Tual, C.; Espuche, E.; Escoubes, M.; Domard, A. *J. Polym. Sci., Part B: Polym. Phys.* **2000**, *38* (11), 1521–1529.
- (19) Roberts, G. A. F.; Taylor, K. E. *Makromol. Chem.* **1989**, *190* (5), 951–960.
- (20) Muzzarelli, R. A. A. *Chitin*; Pergamon Press: Oxford, 1977; p 309.
- (21) Schiffman, J. D.; Schauer, C. L. *Biomacromolecules* **2007**, *8* (2), 594–601.

BM7006983